

High-Resolution Mapping of Surface Morphologies with Focused Ultrasonic Transducers

Thilo M. Brill
Schlumberger
Clamart, France
brill2@slb.com

Melissa Merhej
Schlumberger
Presently: Air Liquide
Sassenage, France
melissa.merhej@gmail.com

Augustin Maller
Schlumberger
Clamart, France
augustin.maller@espci.fr

Jean-Luc Le Calvez
Schlumberger
Clamart, France
JCalvez@slb.com

Christoph Klieber
Schlumberger
Presently: Honeywell
Mainz-Kastel, Germany
contact@klieber.net

Abstract—Using a rotating sensor to take acoustic measurements of geological formations from a fluid-filled borehole is common in the oilfield industry. The deployment of ultrasonic devices enables characterizations of the borehole diameter (caliper) and detailed well bore shape, as well as geological or geomechanical interpretations of formation features such as fractures, rock fabric, stress orientations, failure mechanics and borehole damage. A common mode of operation adopts the ultrasonic pulse-echo technique to achieve a sufficiently high spatial resolution. High-resolution imaging is desirable to improve the ability to discern and characterize morphological features in the borehole surface, which can play a significant role for the production of the reservoir. This paper presents experimental high-resolution investigations using ultrasonic pulse-echo measurements with focused transducers on a range of water-immersed target shapes in a laboratory setup. The targets are composed of combinations of nylon, aluminum, and steel. To facilitate a comparison with numerical modelling, simplified benchmark geometries have been machined into the otherwise planar targets. Here, we report results on notches, cylindrical, and spherical defects. The scanned targets thus represent borehole features, such as borehole breakouts—a form of localized damage of the formation. Fluid-coupled measurements of echo amplitudes and pulse-echo round trip times for 1D or 2D scans were obtained. These scans at nominally vertical incidence were repeated at various sensor standoffs to characterize the response and resolution of the focused transducers. To support the understanding of the spatial sensitivity, numerical acoustic wave field simulations were performed using a k-space pseudo-spectral model of linear elastic wave propagation, available as an open source third party toolbox (named k-Wave®) for MATLAB®. We determine the spatial sensitivity of focused transducers and find a good agreement between the experimental results and the model predictions for these simplified benchmark geometries. We identify the arrival of late echoes after multiple reflections inside of concave recesses and examine how these features can lead to misidentifications of the apparent standoff from the surface without suitable processing.

Index Terms—ultrasonic, pulse-echo, borehole, breakout, fracture, imaging, borehole shape, formation, borehole damage

I. INTRODUCTION

When characterizing deep underground oil and gas wells, a variety of measurement techniques including sonics and ultrasonics are deployed by the industry to evaluate borehole and geological formation properties in-situ [1] - [4]. Common applications include the non-destructive evaluation of the integrity of cement that was pumped in the space

between steel pipes and the rock formation to ensure hydraulic isolation between different fluid- or gas-bearing layers [5] - [8]. Furthermore, borehole imaging is valuable for geological or geomechanical interpretations of formation features such as fractures, rock fabric, stress orientations, failure mechanics and borehole damage [1], [9]. Despite the potentially harsh environmental conditions such as pressures above 1400 bar, temperatures above 175°C and shock levels with accelerations over 100 g, the devices are becoming gradually more sophisticated. To improve efficiency, high-resolution ultrasonic imaging is being deployed already during the drilling operation in combination with other high-resolution measurements [9] - [12]. The identification of fractures is important for formation interpretation due to their role in reservoir production, and their characterization may generally require the combination of different types of high-resolution measurements such as ultrasonics and electrical resistivity [11].

High resolution ultrasonic borehole mapping is typically performed by using a fluid-coupled, focused transducer located on a rotating device and operating in pulse-echo mode [1] - [4]. The round trip travel times and amplitudes of the echoes are determined versus device azimuth and borehole depth. The data can then be presented in the form of 2D images of the formation. The echo amplitudes are affected by the borehole shape, formation rugosity, the presence of scatterers such as rock cuttings, and variations in elastic properties of the rock. Additionally, the properties of the borehole drilling fluid influence the propagation characteristics of the ultrasonic beam. In this context, the borehole fluid attenuation can play a significant role for the device performance since standoff variations translate to undesired echo amplitude variations which may dominate the variations due to formation contrasts. The combination of effects due to device and borehole geometry, fluid dispersion, and formation properties can render the interpretation of travel time and amplitude images challenging. Similar issues were addressed in other industrial applications [13], [14].

In this paper, we report on a series of pulse-echo experiments with focused transducers on a range of water-immersed target shapes in a laboratory setup. The characteristics of these focused transducers which are currently utilized in a prototype device for while-drilling measurements have been

previously described [11]. These sensors have been designed for the purpose high resolution feature imaging with a focused beam spot size of 4 mm at a nominal device standoff to the formation of 25.4 mm in nominal boreholes of 216 mm diameter using an excitation spectrum centered at 375 kHz. In the prototype device the formation is sampled azimuthally every 2° equivalent to a pixel dimension of about 4 mm in nominal boreholes. Previous laboratory results on machined, flat limestone samples have illustrated the sensor response to linear, fracture-like grooves of variable widths. These experiments have demonstrated that the amplitude image resolution is sufficient to identify fine fluid-filled (open) fractures, narrower than 0.5 mm [11]. Excitation spectra centered at lower frequencies can accommodate highly attenuative environments or enlarged borehole sections where image resolution is reduced but a robust borehole caliper can be obtained from the echo travel times.

II. CHOICE OF GEOMETRY AND EXPERIMENTAL METHODS

A. Geometry of the problem

For the laboratory measurements discussed in this report, we direct our attention to formation surface morphologies resembling breakouts, keyseats as well as fractures at oblique angles with respect to the formation surface. Many causes and types of irregular hole shapes can be encountered in a well [1] - [4]. One example is shown schematically in Fig. 1, where a borehole is subject to compressive stresses resulting in possible damage such as induced fractures or breakouts [10] - [12] and [15] - [17]. Alternatively, a borehole may intersect a preexisting fracture plane or discontinuity. Depending on their geological history, fractures can be fluid-filled (open) or composed of a solid with different elastic properties from the host formation. The orientation of fracture planes can be at arbitrary angles with respect to the borehole (and sensor) axis. In the cases of drilling-induced damage such as breakouts or keyseats [4] the borehole becomes locally enlarged (see Fig. 1). Keyseat-type formation damage is due to erosion by the motion of the drillpipe.

For the targets of our pulse-echo experiments we adopted a simplified geometry of planar, layered media. This approach can be justified based on the nearly flat borehole interface on the scale of the ultrasonic beam spot size (4 mm) relative to the nominal borehole radius of 108 mm. Furthermore, borehole pulse-echo measurements while drilling typically only determine travel times and amplitudes of the time-gated first echo in a waveform. This usually corresponds to the shortest round trip path between the transducer and the formation surface. Thus, no information of more distant or deeper scattering events are exploited. This limits effects of 3D interactions, interference or multiple scattering. Finally, the planar geometry allows for simplified numerical modelling in 2D to capture the essential interactions which contribute to the echo waveform. However, for a quantitatively accurate description of the focused acoustic beam a 3D model is required.

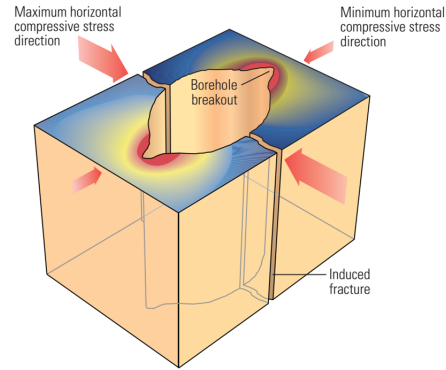


Fig. 1. Schematic view of a vertical borehole through a formation. Anisotropic stress distributions may cause borehole damage in the form of induced fractures or breakouts.

B. Set-up

Fig. 2 depicts the transducer and target in a typical experimental setup. We used spatially highly resolved scans along the y-direction for a given standoff (x-direction) across a target surface and detect pulse-echo waveforms. The envelope amplitude of waveform signals and the associated travel time were extracted for an excitation spectrum centered at 375 kHz.

The water-immersed target materials in our laboratory measurements are aluminum and nylon. Table 1 lists elastic properties used in our modelling which include compressional velocity (V_p), shear velocity (V_s) and density. The pulse-echo specular reflection coefficients of a flat interface are a function of the acoustic impedance Z (the product of density and V_p) contrasts at the interface between water and target material. In comparison, rock formation acoustic impedances roughly span a range of 3 MRayl to 19 MRayl [1].

For breakout or keyseat-type morphologies we used nylon targets as shown schematically in Fig. 2. Experiments were performed in geometries with cylindrical or highly localized spherical cutouts in the nylon host target.

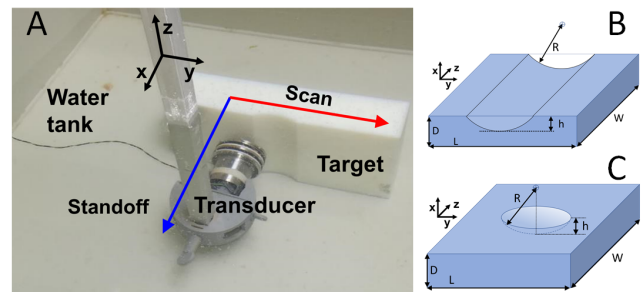


Fig. 2. Experimental setup and schematic targets. A) The transducer is shown attached to a water-immersed arm of an xy linear translation stage. The picture shows the transducer in pulse-echo arrangement, oriented parallel to the x-axis and facing a nylon target at normal incidence. In this configuration scans are performed along the y direction across the target surface for various standoffs in x direction. B) Schematic view of a nylon target with a cylindrical cutout. C) Schematic view of a nylon target with a spherical cutout. The nylon targets have dimensions $L = 200$ mm \times $W = 100$ mm \times $D = 40$ mm.

TABLE I
MATERIAL PROPERTIES

Material	V_p (m/s)	V_s (m/s)	Density (kg/m ³)	Z (MRayl)
Water	1500	0	1000	1.5
Aluminium	6450	3100	2700	17.4
Nylon	2630	1150	1180	3.1

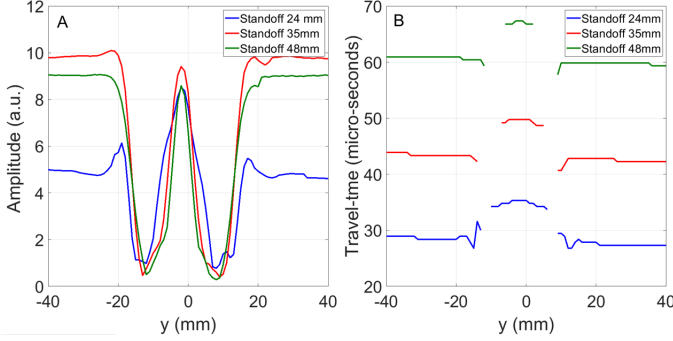


Fig. 3. Experimental pulse-echo results for scans along the y -direction across a nylon target with cylindrical cutout as depicted in Fig. 2. The cutout has a radius of $R = 25$ mm and a penetration depth of $h = 5$ mm. The scan positions are sampled at 1 mm increments. The center of the cutout is located at scan position $y = -2$ mm. Results are shown for three different sensor standoff's (along the x -direction) between transducer and the flat section of the target. The left figure (A) shows the echo amplitudes in arbitrary units for standoff's indicated in the legend. The right graph (B) shows the corresponding measured travel times. Gaps in the travel time measurements correspond to multiple reflections and are not shown for clarity.

To represent fracture-like discontinuities or thin layers in a formation that intersect the borehole at different angles we created a gap of variable dimensions between two aluminum blocks. We machined block pairs with varying angles α of the gap orientation relative to the surface normal. By sliding the two blocks on a flat aluminum surface the matching surfaces remain mutually parallel and the gap width d of the discontinuity and the resulting opening aperture AP can be controlled.

The numerical time domain modeling was performed with the open source MATLAB toolbox k-Wave [18]. The simulation is based on a k -space pseudo-spectral time domain solution to coupled first-order acoustic equations for homogeneous or heterogeneous media.

III. RESULTS

A. Breakout or keyseat-type features

1) *Cylindrical target*: An example of the experimental results for a nylon target with a cylindrical cutout defined by a radius of $R = 25$ mm and a penetration depth of $h = 5$ mm are given in Fig. 3. The surface aperture of the cutout is 30 mm wide. Three standoffs of the sensor from the flat target surface have been selected, 24 mm, 35 mm and 48 mm.

A few characteristic features can be noted: First, the pulse-echo amplitudes facing the flat section of the target exhibit a maximum near 35 mm standoff which is in the focal zone of the focused transducer (Fig. 3 A). Second, for the amplitude

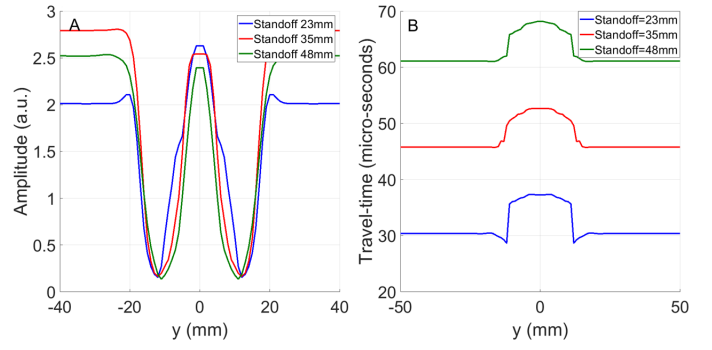


Fig. 4. Numerical simulation results in 2D corresponding to the experimental data of Fig. 3. The left figure (A) shows the echo amplitudes (in arbitrary units) for standoffs indicated in the legend. The right graph (B) shows the corresponding round trip travel times.

measurements the lateral dimension of the cylindrical cutout appears slightly larger than 30 mm. This is due to the convolution of the sensor spatial response function with the geometrical features of the target. Third, both amplitude and travel time (Fig. 3 B) measurements can exhibit pronounced overshoots near the edges of the cutout. These are diffraction related effects and can give false halo-type borehole image distortions around sharp geometrical contrasts. An additional complication for the interpretation of these overshoots is that they also depend on the sensor standoff. Fourth, the echo amplitudes near the inner perimeter of the cylindrical cutouts are strongly reduced because the specularly reflected beam is directed away from the transducer. This is associated with a poorly defined travel time (Fig. 3 B). In particular, without appropriate time gating of the echo peaks this scenario is prone to the detection of late-arriving echoes from more distant scatterers or after multiple scattering. On borehole images these areas can be difficult to interpret correctly. Finally, due to the perfectly cylindrical shape of the cutout which acts like a refocusing mirror a strong backscattering peak is observed above the center of the defect.

In Fig. 4 we show numerical results corresponding to the experiments of Fig. 3. The amplitudes (Fig. 4 A) and travel times (Fig. 4 B) exhibit the same characteristics as described above for the experimental results and the overall agreement is satisfactorily.

2) *Two-dimensional imaging* : The experimental results shown in Fig. 5 show amplitude and travel time images for a 2D high-resolution scan across the surface of a nylon block with a spherical cutout of radius $R = 25$ mm and penetration depth of $h = 5$ mm (see Fig. 2 C). The aperture diameter of the circular cutout is 30 mm. The standoff was fixed at 38 mm from the flat section of the target. As already seen in the cross-section of the target with a cylindrical cutout (Fig. 3) one can identify the halo-type distortion around the perimeter of the circular cutout opening due to amplitude overshoots in Fig. 5 A. These are diffraction effects around sharp geometrical contrasts. The effect is not present in the

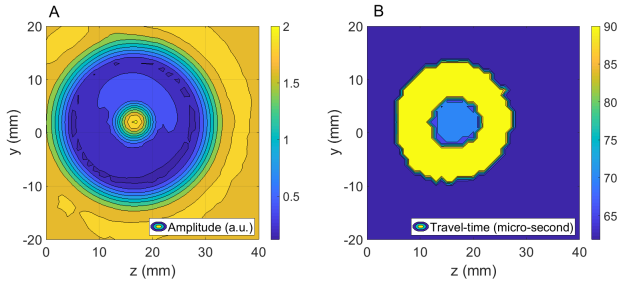


Fig. 5. Experimental pulse-echo imaging results for scans along the y- and z-direction across a nylon target with spherical cutout as depicted in Fig. 3 B. The cutout has a radius of $R = 25$ mm and a penetration depth of $h = 5$ mm. The scan positions are sampled at 1 mm increments in both y and z directions. Results are shown for a sensor standoff (in x-direction) of 38 mm between transducer and the flat section of the target. The left image (A) shows the echo amplitudes as a colorscale in arbitrary units. The right image (B) shows the corresponding measured travel times.

travel time image of Fig. 5 B. However, the difficulty of determining a robust travel time near the inner perimeter of the spherical cutout affects the apparent size of the cutout opening which appears only about 20 mm wide in Fig. 5 B. In fact, one can observe that the travel times near the perimeter of the cutout exhibit strong discontinuities. Hence the appearance of a disc of much longer travel times than at the center of the target. Those are associated with late-arriving echoes after two specular reflections inside the spherical defect.

B. Fracture type features

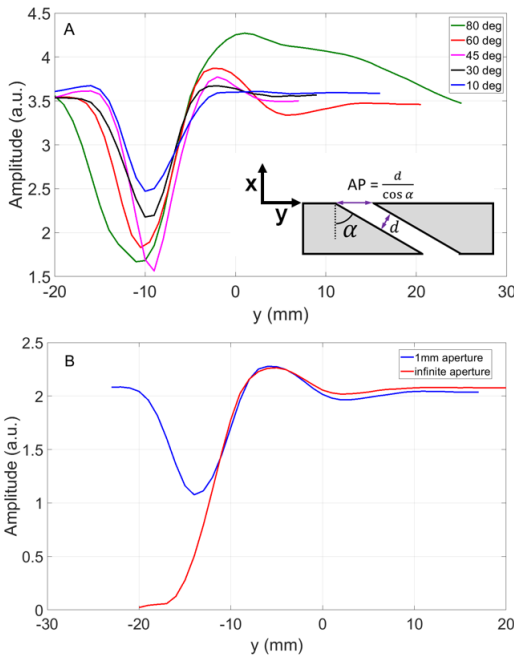


Fig. 6. Experimental pulse-echo amplitude results for scans along the y-direction across an aluminium target with oblique water-filled gap. (A) The angle α increases from 10° to 80° . The gap tilts towards positive values of the y-direction. In (B) the angle is fixed at 60° and the 1 mm aperture is compared to an isolated block simulating an infinite aperture.

In Fig. 6 A we show one set of amplitude measurements for a fixed standoff (along the x direction) of 38 mm. The aperture of the gap is about $AP = 1$ mm, thus only about a quarter of the wavelength in water at 375 kHz.

We find that the amplitude is symmetrically reduced above the gap for near-vertical angles $\alpha < 10^\circ$. As the angle increases, a clear asymmetry develops with an enhancement of the amplitude towards positive y. This amplitude enhancement does not strongly depend on the aperture width as demonstrated in Fig. 6 B. However, the asymmetric amplitude variation increases with gap angle α and reaches about 20% of the background level at $\alpha = 80^\circ$. This asymmetric amplitude enhancement is due to contributions to the time-gated first echo signal from refracted and reflected pathways inside the section of formation with the acute angle and depends on the distance from the fracture aperture.

This observation indicates that fluid-filled fractures which intersect a borehole at oblique angles may exhibit an amplitude image distortion compared to the nominal formation amplitude. In this case, an increase of the echo amplitude adjacent to the feature does not necessarily indicate any intrinsic changes of the elastic properties of the rock but could be a possible indicator for an oblique fracture plane angle.

IV. CONCLUSION

The aim of the experimental investigation is the pulse-echo imaging with focused transducers of surface morphologies resembling breakouts, keyseats and fractures at oblique angles with respect to a flat formation surface. High-resolution laboratory experiments were performed using simplified geometries to better characterize and understand the interaction of focused ultrasonic beams in a borehole environment. We also used numerical modeling to further our understanding of the underlying mechanisms of reflections and diffraction effects at the interface between borehole fluid and formation surface. We find that echo amplitude and travel time measurements can exhibit pronounced diffraction related distortions near sharp geometrical discontinuities. Due to the focused transducer beam profile these image artefacts typically depend on the transducer standoff from the formation. Amplitude and travel time measurements exhibit different sensitivities to the presence of these geometrical discontinuities. Without appropriate processing, borehole images may be difficult to interpret as concave surface morphologies favor the detection of late-arriving echoes from more distant scatterers or after multiple scattering. Finally, cases of fluid-filled fractures which intersect a borehole at oblique angles were found to exhibit asymmetric amplitude image distortions which are indicative of the fracture plane angle. If not recognized correctly, the observed image distortions could lead to misinterpretations.

ACKNOWLEDGMENT

The authors would like to thank Jean-Christophe Auchere for the support of this project, Carlos Maeso for many stimulating discussions, Orland Guedes and Fabrice Mege for their support with the experimental setup.

REFERENCES

- [1] D. Ellis, J. Singer, *Well Logging for Earth Scientists*, 2nd ed., Springer, 2008.
- [2] C. P. Gooneratne, B. Li, M. Deffenbaugh, and D.T. Moellendick, *Instruments, Measurement Principles and Communication Technologies for Downhole Drilling Environments, Smart Sensors, Measurement and Instrumentation book series*, vol. 32, 2019.
- [3] S. Zeroug and S. Bose, "Recent advances in the use of acoustics across the frequency spectrum in the oil and gas industry," *AIP Conference Proceedings*, vol. 1949, 020014, 2018.
- [4] A.J. Hayman, P. Parent, P. Cheung, and P. Verges, "Improved Borehole Imaging by Ultrasonics," *SPE Production & Facilities*, vol. 13, pp. 514, 1998.
- [5] S. Thierry et al., "Ultrasonic cement logging: Expanding the operating envelope and efficiency," *SPWLA 58th Annual Logging Symposium*, Oklahoma City, June 2017.
- [6] T.M. Brill and C. Klieber, "Reflection and mode-conversion of ultrasonic Lamb waves at inaccessible discontinuities in layered structures," *IEEE International Ultrasonics Symposium*, Tours, September 2016.
- [7] C. Klieber, S. Catheline, Y. Vincensini, T.M. Brill, and F. Mege, "Visualization of leaky ultrasonic Lamb wave experiments in multilayer structures, International Congress on Ultrasonics," *Physics Procedia*, vol. 70, pp. 314317, 2015.
- [8] C. Klieber, T.M. Brill, M. Lemarenko, and S. Catheline, "Effect of microannulus on ultrasonic pulse-echo resonance and flexural Lamb-wave cement-evaluation measurements," *Proceedings of Meetings on Acoustics*, vol. 30, 065014, 2017.
- [9] S. Zeroug, B.K. Sinha, T. Lei, and J. Jeffers, "Rock heterogeneity at the centimeter scale, proxies for interfacial weakness, and rock strength-stress interplay from downhole ultrasonic measurements," *Geophysics*, vol. 83, no. 3, pp. D83-D95, 2018.
- [10] H. Dollfus, H.-P. Valero, J.-C. Auchere, and H. Hori, "Automatic Estimation of Borehole Shape Using Ultrasonic Data While Drilling," *IEEE International Ultrasonics Symposium (IUS)*, October 2018
- [11] C.J. Maeso et al., "Field Test Results of a New High-Resolution, Dual Physics Logging-While-Drilling Imaging Tool In Oilbase Mud," *SPWLA 59th Annual Logging Symposium*, June 2018.
- [12] N. Ritzmann et al., "High-Resolution LWD Acoustic Borehole Imaging in WBM and OBM," *14th Offshore Mediterranean Conference and Exhibition*, Ravenna, Italy, March 2019.
- [13] M.V. Felice and Z. Fan, "Sizing of flaws using ultrasonic bulk wave testing: A review," *Ultrasonics*, Vol. 88, pp. 2642, 2018.
- [14] L. Su, X. Yu, K. Li, X. Yao, M. Pecht, "Simulation and Experimental Verification of Edge Blurring Phenomenon in Microdefect Inspection Based on High-Frequency Ultrasound," *IEEE Access*, Vol. 7, pp. 11515-11525, 2019.
- [15] C.J. Maeso et al., "Fracture Aperture Calculations From Wireline and Logging While Drilling," *Proceedings of the SPE Annual Technical Conference and Exhibition*, Amsterdam, The Netherlands, October 2014.
- [16] E. Simsek, B.K. Sinha, S. Zeroug, and N. Bounoua, "Influence of break-outs on borehole sonic dispersions," *77th SEG International Exposition and Annual Meeting*, Society of Exploration Geophysicists, 2007.
- [17] M.D. Zoback et al., "Determination of stress orientation and magnitude in deep wells," *International Journal of Rock Mechanics and Mining Sciences*, Vol. 40, no. 78, pp. 1049-1076, 2003.
- [18] B.E. Treeby and B.T. Cox, "k-Wave: MATLAB toolbox for the simulation and reconstruction of photoacoustic wave fields," *J. Biomed. Opt.*, Vol. 12, no. 2, 021314, 2010.